Journal of the Korean Astronomical Society
50: 151 ∼ 155, 2017 October

http://dx.doi.org/10.5303/JKAS.2017.50.5.151
pISSN: 1225-4614 · eISSN: 2288-890X
http://jkas.kas.org

Low Frequency Observations of a Radio Loud Dwarf Galaxy

Songyoun Park[1], Chandreyee Sengupta[2], Bong Won Sohn[3], and Sanjaya Paudel[4]
[1]Department of Physics and Astronomy, Seoul National University, Gwanak-gu, Seoul 08826, Korea; sypark@astro.snu.ac.kr
[2]Yonsei University Observatory, Yonsei University, 50 Yonsei-ro, Seodaemun-gu, Seoul 03722, Korea sengupta.chandreyee@gmail.com
[3]Korea Astronomy and Space Science Institute, 776 Daedukdae-ro, Yuseong-gu, Daejeon 34055, Korea; bwsohn@kasi.re.kr
[4]Department of Astronomy & Center for Galaxy Evolution Research, Yonsei University, 50 Yonsei-ro, Seodaemun-gu, Seoul 03722, Korea; sanjpaudel@gmail.com

Received May 10, 2017; accepted September 22, 2014

Abstract: We investigate the radio properties of the dwarf galaxy SDSS J133245.62+263449.3 which shows optical signatures of black hole activity. Dwarf galaxies are known to host intermediate mass black holes (IMBHs) with masses $M_{\rm BH} \sim 10^{4-6} M_\odot$, some of them being radio loud. Recently, Reines et al. (2013) found dwarf galaxy candidates which show signatures of being black hole hosts based on optical spectral lines. SDSS J133245.62+263449.3 is one of them; it shows a flux density of $\sim$ 20 mJy at 1.4 GHz, which corresponds to $L_{\rm 1.4GHz} \sim 10^{23}\,{\rm W\,Hz^{-1}}$. This is much brighter than other black hole host dwarf galaxies. However, star formation activity can contribute to radio continuum emission as well. To understand the nature of the radio emission from SDSS J133245.62+263449.3, we imaged this radio loud dwarf galaxy at low frequencies (325 MHz and 610 MHz) using the Giant Metrewave Radio Telescope (GMRT). We present here the high resolution images from our GMRT observations. While we detect no obvious extended emission from radio jets from the central AGN, we do find the emission to be moderately extended and unlikely to be dominated by disk star formation. VLBI observations using the Korean VLBI Network (KVN) are now being planned to understand the emission morphology and radiation mechanism.

Key words: galaxies: dwarf — galaxies: active — black hole physics — techniques: interferometric

1. Introduction

Supermassive black holes with masses $M_{\rm BH} \sim 10^{6-9} M_\odot$ are common at the centers of massive galaxies (**?**). Dwarf galaxies, on the other hand, are thought to host intermediate mass black holes (IMBH) with $M_{\rm BH} \sim 10^{4-6} M_\odot$ in their centers (**?**). In radio wavelengths, it is difficult to detect signs of black hole activity in dwarf galaxies in the distant as well as nearby universe because of their low luminosities, which is usually dominated by star formation. However, radio observations of black hole host dwarf galaxies are worth pursuing as they can reveal information related to the formation and growth of the seed black holes as well as the properties of the host galaxies of which very little is known to us.

To date, only a few low-mass dwarf galaxies like Pox 52, a dwarf elliptical (**?**), and NGC 4395, a bulgeless spiral galaxy with a nuclear star cluster (**?**), have been reported to be hosting black holes, primarily IMBHs. Another accreting IMBH was found at the center of Henize 2-10 through a multi-wavelength study (**?**). This dwarf starburst galaxy is nearby, gas-rich, and has super-star clusters that host a young and massive stellar population. In addition to these individual discoveries, a systematic study of black holes was attempted using SDSS data where ∼200 broad-line AGNs with black hole masses of $10^{5-6} M_\odot$ were found by **??**. **?** searched for narrow-line AGNs with low stellar velocity dispersions ($39 < \sigma < 94$ km s^{-1}), which can indicate the presence of low-mass black holes. However, most of the sample galaxies in the previous studies have typical stellar masses of $M_\star \sim 10^{10} M_\odot$, well above the dwarf galaxy regime.

Recently, a systematic search for optical AGN activity in dwarf galaxies was carried out by **?**. They present a sample of 151 dwarf galaxies with stellar mass $\sim 10^{8.5-9.5} M_\odot$ using SDSS spectroscopic data. Their sample selection was based on emission line ratios in order to examine whether optical emission is dominated by star formation or AGN activity. We compared this sample with radio surveys such as the Faint Images of the Radio Sky at Twenty-cm (FIRST) and the NRAO VLA Sky Survey (NVSS), and identified a subset of dwarf galaxies with radio counterparts. In this paper we present Giant Metrewave Radio Telescope (GMRT) low frequency, 325 MHz and 610 MHz, interferometric observations of SDSS J133245.62+263449.3, the dwarf galaxy from the Reines et al. (2013) sample with the highest flux (∼21 mJy) at 1.4 GHz. Our observations were carried out to understand the low frequency emission and to search for extended jets at low frequencies, a feature unlikely to be associated to dwarf galaxies. The heliocentric radial velocity of SDSS J133245.62+263449.3 as quoted in the NASA Extra-

Corresponding author: B. W. Sohn

Table 1
Details for the two GMRT observations

Frequency	325 MHz
Observation Date	January 4, 2015
R.A. (pointing centre)	$13^{\rm h}$ $32^{\rm m}$ $45.6^{\rm s}$
DEC (pointing centre)	$26°$ $34^{\rm m}$ $49.3^{\rm s}$
Primary calibrator	3C 286
Phase calibrator	3C 286
Integration time	3.5 hrs
Primary beam	$81'$ at 325 MHz
Beamsize	$12.7'' \times 8.4''$ (PA = 80.7°)
Map rms	0.40 mJy beam^{-1}
Frequency	610 MHz
Observation Date	November 27, 2014
R.A. (pointing centre)	$13^{\rm h}$ $32^{\rm m}$ $45.6^{\rm s}$
DEC (pointing centre)	$26°$ $34^{\rm m}$ $49.3^{\rm s}$
Primary calibrator	3C 286
Phase calibrator	3C 286
Integration time	3.5 hrs
Primary beam	$43'$ at 610 MHz
Beamsize	$6.1'' \times 5.4''$ (PA = -69.8°)
Map rms	0.14 mJy beam^{-1}

galactic Database (NED) is 14 092 km s^{-1}. Assuming H_0 to be 70 km s^{-1} Mpc^{-1}, we estimate the distance to the galaxy to be ∼200 Mpc.

2. Observations and Data Analysis

2.1. Radio Data: GMRT and FIRST

Low frequency radio continuum observations at 325 MHz and 610 MHz were carried out using the Giant Metrewave Radio Telescope (GMRT)[1] on January 4, 2015 and November 27, 2014, respectively. Baseband bandwidths were 16 and 33 MHz at 325 MHz and 610 MHz, respectively. Further details of the observations are listed in Table 1. We used the 'Astronomical Image Processing System' (`AIPS`) software package for data reduction. Flux densities were calibrated using the **?** scale, with flux density uncertainties of ∼5%. Bad data were flagged, the remaining data were calibrated and imaged. The `AIPS` task `IMAGR` was used to make the final 'clean' images. The wide field imaging option was applied to both frequencies and the data were self-calibrated before the final images were prepared. In this paper, we present the high resolution images produced by using the uv-range and uniform weighting options in the `IMAGR` program. We used the 1.4 GHz (20 cm) continuum data from the Faint Images of the Radio Sky at Twenty-cm (FIRST) survey. FIRST is a high resolution ($\sim 5''$) 20-cm continuum interferometric imaging survey carried out using the NRAO Very Large Array (VLA) in B configuration. Images from the survey are available online.[2]

[1] `http://gmrt.ncra.tifr.res.in`
[2] `http://sundog.stsci.edu/first/images.html`

2.2. Optical Data: Archived SDSS Spectrum

We performed spectral decomposition using an archived SDSS DR7 spectrum (**?**) of SDSS J133245.62+263449.3 to search for broad line emission. We followed the methodology by **?** to decompose the line components. For model fitting we used the nonlinear Levenberg-Marquardt least-squares fitting routine `MPFIT` (**?**) in `IDL`. We subtracted the AGN continuum from the SDSS spectrum using a power-law model continuum. The continuum model was fitted to the observed flux in the spectral regions 4430–4600 Å, 5080–5550 Å, 6400–6460 Å, and 6740–6800 Å where line emission is irrelevant. In the continuum-subtracted spectrum, we modeled emission lines such as Hα, Hβ, and [O III] $\lambda\lambda$4959, 5007 by fitting Gaussian model profiles to the data (see Figure 1). The flux ratio of [O III] λ4959 and [O III] λ5007 was assumed to be 1:3. As **?** already suggested, our target did not exhibit any prominent broad component of either Hα or Hβ.

3. Results

3.1. Results from Radio Observations

The three panels of Figure 2 show the high resolution GMRT low frequency images along the FIRST 1.4-GHz image of SDSS J133245.62+263449.3. From left to right, the first and the second panel show the GMRT 325 MHz and 610 MHz intensity contours (in black) overlayed on the SDSS g–band optical map. The third panel shows the FIRST 1.4-GHz contours overlayed on the same SDSS g–band map. The synthesized beams are plotted in the lower left corner of each map. The emission shows no clear structure. The emission is marginally extended; there is no lobe-like structure.

The spectral index α is defined as $S_\nu \propto \nu^\alpha$, where S_ν is the flux density and ν is the observing frequency. We estimated the spectral index from the flux density measurements at 325 MHz (∼45.5 mJy), 610 MHz (∼36.4 mJy) and 1.4 GHz (∼21.0 mJy). The spectral index is −0.6, suggesting that the spectrum is dominated by non-thermal emission as expected in normal spiral galaxies.

3.2. Star Formation Rate

We estimated star formation rates (SFRs) in three different wavelength regimes: FUV (GALEX), Hα (SDSS), and radio (FIRST), using the conversion equations

$$\mathrm{SFR_{FUV}}(/M_\odot \mathrm{yr}^{-1}) = 1.27 \times 10^{-28} \times \mathrm{L_{FUV}}(/\mathrm{erg\ s^{-1} Hz^{-1}}) \quad (1)$$

$$\mathrm{SFR_{H\alpha}}(/M_\odot \mathrm{yr}^{-1}) = 6.9 \times 10^{-42} \times \mathrm{L_{H\alpha}}(/\mathrm{erg\ s^{-1}}) \quad (2)$$

$$\mathrm{SFR_{1.4GHz}}(/M_\odot \mathrm{yr}^{-1}) = 0.75 \times 10^{-21} \times \mathrm{L_{1.4GHz}}(/\mathrm{W\ Hz^{-1}}) \quad (3)$$

(**??**). The total H$_\alpha$ emission line flux measured from the SDSS spectrum is 1.42×10^{-14} erg cm^{-2} s^{-1} whereas the GALEX FUV flux is 1.7×10^{-15} erg cm^{-2} s^{-1} Å^{-1}. The SFR estimated from FUV and Hα using Equations (**??**) and (**??**) is 0.7 $M_\odot$ yr^{-1} and 0.4 $M_\odot$ yr^{-1}, respectively. However, the SFR estimated from the

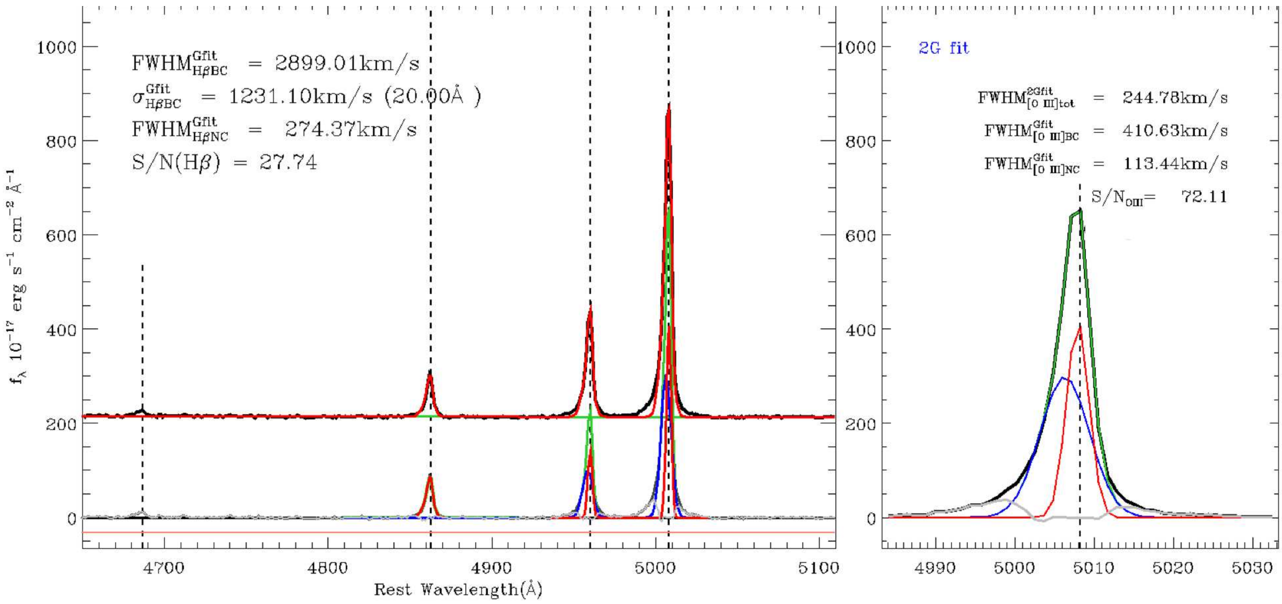

Figure 1. Spectral decomposition of Hβ and [O III] emission lines. We employed Gaussian profiles to model the emission lines after removing a power law continuum. *Left panel:* Fits using one and two line components in the top and and bottom plot, respectively. The black and green lines are observed spectrum and power-law continuum, respectively, where orange denotes the best-fit one-component emission line plus power-law continuum. We show the best-fit two-component Gaussian emission lines in red and blue color (lower plot), where the green line represents the sum of both. The gray line is the residual (observation − best fit). The right panel is a zoom view onto the wavelength region 4990–5030 Å.

radio flux density at 1.4 GHz is two orders of magnitude higher, 71 $M_\odot$ yr^{-1}. Star formation rates of dwarf galaxies show a wide range from $\sim10^{-4}$ to ~1 $M_\odot$ yr^{-1} (**???**). Thus the FUV and Hα SFRs of SDSS J133245.62+263449.3 can be considered to be on the high side. The SFR estimated using the 1.4 GHz flux density clearly indicates that the majority of the radio emission is from the central engine of the galaxy and not from star formation.

3.3. Black Hole Mass and Eddington Ratio

Since a broad Hβ component was not found for our target, the black hole mass was derived from the [O III] emission line width using the equation (**?**)

$$\log\left(M_{\mathrm{BH}}/M_\odot\right) = (3.7\pm0.7)\log\left(\mathrm{FWHM}_{[\mathrm{O\,III}]}/2.35\right) + (-0.5\pm0.1) \quad (4)$$

where $\mathrm{FWHM}_{[\mathrm{O\,III}]}$ is the full width at half maximum of the [O III] $\lambda5007$ emission line which is $\sim$274 km s-1. The estimated black hole mass is $9.3\times10^7 M_\odot$. The Eddington luminosity was calculated from the relation $L_{\mathrm{Edd}} = 1.25\times10^{38}(M_{\mathrm{BH}}/M_\odot)$ erg s^{-1} (**?**). We measured the optical continuum luminosity at 5100 Å (L_{5100}) and applied the bolometric correction $L_{\mathrm{bol}} = 10.3\lambda L_{5100}$ (**?**). The Eddington ratio is 0.061, which indicates a low level of mass accretion onto the central black hole.

4. Discussion

Searching for radio loud AGNs in dwarf galaxies, we found the dwarf galaxy SDSS J133245.62+263449.3 to be very bright in radio with a 1.4-GHz flux of $\sim$21 mJy. The optical major axis diameter of the galaxy as obtained from the NASA/IPAC Extragalactic Database (NED) is 0.19′. At 200 Mpc, this translates to $\sim$ 10 kpc. The stellar mass of the galaxy is $\sim 2.45\times10^9 M_\odot$ (**?**). The galaxy is quite isolated: the nearest neighbour with similar redshift is about 20′ away, corresponding to $\sim$1 Mpc. SDSS J133245.62+263449.3 was listed as a dwarf galaxy with optical signatures of an AGN and as a massive black hole host by **?**. Their work was the first systematic statistical study aimed at understanding the AGN population in dwarf galaxies. Using SDSS spectra, they identified and produced a list of dwarf galaxies with narrow-line photoionization signatures of accreting massive black holes. In addition, they looked for broad Hα emission signatures from gaseous material orbiting the central massive black hole, which would help estimate the black hole mass (**?**). To distinguish AGNs from normal star formation related emission from H II regions, **?** (BPT) diagrams were used; there, SDSS J133245.62+263449.3 qualified as an AGN dominated system. The log(N II/Hα) and log(O III/Hβ) values were estimated to be −0.34 and 0.86, respectively. No broad Hα or Hβ line emission was detected in the SDSS spectrum by **?**. We reanalyzed the SDSS spectrum (following the procedure in Section 2.2) and confirmed the absence of broad line emission. Since a broad line component was not detected in our target, we estimated the black hole mass using the [O III] emission line (Section 3.3). The estimated black hole mass is $\sim 9.3\times10^7 M_\odot$. This is higher than expected for an IMBH and given the optical mass of the dwarf galaxy

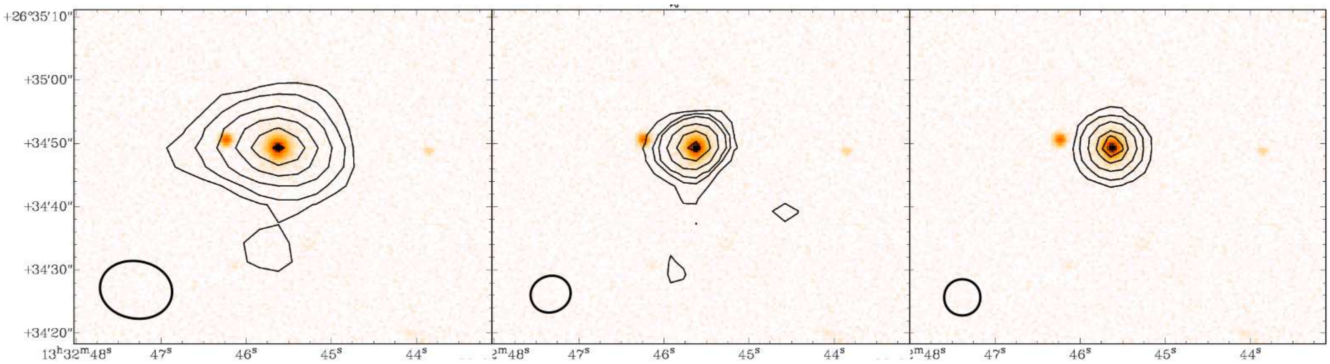

Figure 2. GMRT low frequency (325MHz and 610 MHz) and FIRST 1.4 GHz images of SDSS J133245.62+263449.3. Beams are plotted in the lower left corner of each image. *Left panel:* GMRT 325 MHz-image overlayed on SDSS g-band image. The contour levels are (2, 5, 10, 20, 30, 40) mJy beam^{-1}. *Middle panel:* GMRT 610-MHz image overlayed on SDSS g-band image. The contour levels are (0.6, 1, 3, 10, 20, 30) mJy beam^{-1}. *Right panel:* FIRST 1.4-GHz image overlayed on SDSS g-band image. The contour levels are (1.5, 3, 5, 10, 15, 19) mJy beam^{-1}.

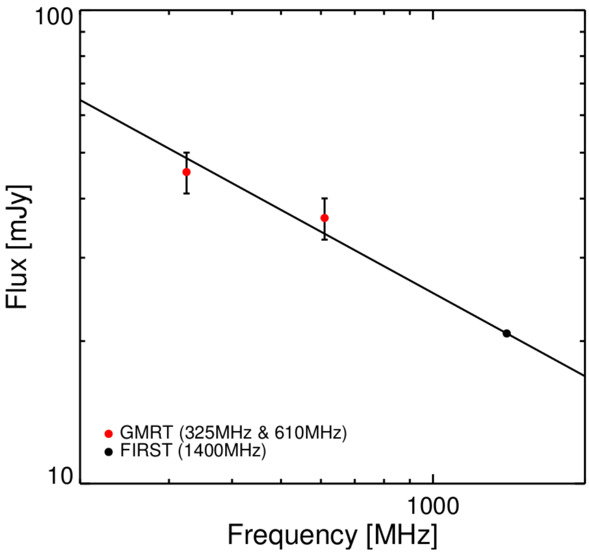

Figure 3. Spectral index measurement, using the integrated flux densities at 325 MHz, 610 MHz, and 1.4 GHz.

of $\sim 2.5 \times 10^9 M_\odot$.

Amongst all the 151 dwarf galaxies that exhibit optical spectroscopic signatures of accreting massive black holes in **?**, SDSS J133245.62+263449.3 is the brightest at 1.4 GHz. It is also much brighter than other well-known dwarf galaxies hosting IMBHs, such as Henize 2-10 ($L_{1.4\mathrm{GHz}} \sim 10^{19}$ W Hz^{-1}, **?**) and NGC 4395 ($L_{1.4\mathrm{GHz}} \sim 10^{18}$ W Hz^{-1}, **?**). Having found a radio-loud AGN-dominated dwarf galaxy in the literature, we carried out low-frequency radio imaging with the GMRT, primarily to detect any extended structures like radio jets or lobes. The 1.4-GHz integrated flux of this galaxy in the FIRST and the NVSS is similar within errors, 20.8 mJy and 21.7 mJy respectively. Despite the difference in angular resolution between the surveys, the flux remains similar, suggesting compactness. However, a closer look at Figure 2 (right panel) shows that even the FIRST beam ($\sim 5''$) does not ensure that the radio emission originates from the central engine, leaving the possibility of some contribution from disk star formation activity or the presence of small-scale radio jets.

The moderately extended nature of the radio emission is also seen in the GMRT images in 325 MHz and 610 MHz, though no signature of radio lobes or jets could be detected. Lack of spatial resolution prevents us from making a spectral index (SI) map of the galaxy, however the global SI gives some hints about the nature of the radio emission. The SI from the integrated flux density of the galaxy in the three bands (325 MHz, 610 MHz, and 1.4 GHz) is $\alpha \approx -0.6$, indicating that the emission is predominantly non-thermal in nature (Figure 3). However, α seems to be marginally shallower than the expected average value (about -0.7 to -0.8) found in normal spiral galaxies (**?**). A possible explanation would be thermal emission from star formation activity at 1.4 GHz. The galaxy exhibits bright UV emission in the GALEX All Sky Survey; its SFR estimated from FUV (GALEX) and Hα (SDSS) are 0.7 $M_\odot$ yr^{-1} and 0.4 $M_\odot$ yr^{-1}, respectively. Given its morphology and size as well as the fact that the usual range of SFR found in dwarf galaxies is $\sim 10^{-4}$ to $1 M_\odot$ yr^{-1} (**???**), the SFR of this galaxy can be considered marginally higher than average. In contrast, the SFR estimated using the radio flux density at 1.4 GHz turns out to be two orders of magnitude higher, 71 $M_\odot$ yr^{-1}. This discrepancy indicates that the radio emission at 1.4 GHz must be dominated by a central source. However, while we do detect modest extended emission from the galaxy in all low-frequency bands (from 325 MHz to 1.4 GHz), which is unlikely to be contributed by disk star formation, no clear signature of radio jets was detected.

To summarize, our GMRT low-frequency imaging of SDSS J133245.62+263449.3 hints towards the presence of small-scale jets from the AGN in the galaxy. However, even with the highest available resolution in these frequencies (325MHz and 610 MHz) offered by any current radio interferometer, we could not detect clear signatures of radio jets or lobes or any significant structure in the emission. We are now planning VLBI observations using the Korea VLBI Network (KVN) to estimate the compactness of the source and to probe possible small-scale jet signatures.

Acknowledgments

We thank the staff of the GMRT who have made these observations possible. The GMRT is operated by the National Centre for Radio Astrophysics of the Tata Institute of Fundamental Research. C. Sengupta acknowledges support for this work by the Science Fellowship of POSCO TJ Park Foundation. S. Paudel acknowledges the support by Samsung Science & Technology Foundation under Project Number SSTF-BA1501-0. B. W. Sohn is grateful for the support of the National Research Council of Science and Technology, Korea (Project Number EU-16-001). This research has made use of the NASA/IPAC Extragalactic Database (NED) which is operated by the Jet Propulsion Laboratory, California Institute of Technology, under contract with the National Aeronautics and Space Administration. This research has made use of the Sloan Digital Sky Survey (SDSS). Funding for the SDSS and SDSS-II has been provided by the Alfred P. Sloan Foundation, the Participating Institutions, the National Science Foundation, the U.S. Department of Energy, the National Aeronautics and Space Administration, the Japanese Monbukagakusho, the Max Planck Society, and the Higher Education Funding Council for England. The SDSS web site is `http://www.sdss.org`. This research made use of APLpy, an open-source plotting package for Python hosted at `http://aplpy.github.com`.

References

Abazajian, K. N., Adelman-McCarthy, J. K., Agüeros, M. A., et al. 2009, The Seventh Data Release of the Sloan Digital Sky Survey, ApJS, 182, 543

Baars J. W. M., Genzel, R., Pauliny-Toth, I. I. K., & Witzel, A. 1977, The Absolute Spectrum of Cas A – An Accurate Flux Density Scale and a Set of Secondary Calibrators, A&A, 61, 99

Baldwin, J. A., Phillips, M. M., & Terlevich, R. 1981, Classification Parameters for the Emission Line Spectra of Extragalactic Objects, PASP, 93, 5

Barth, A. J., Ho, L. C., Rutledge, R. E., & Sargent, W. L. W. 2004, POX 52: A Dwarf Seyfert 1 Galaxy with an Intermediate-Mass Black Hole, ApJ, 607, 90

Barth, A. J., Greene, J. E., & Ho, L. C. 2008, Low-Mass Seyfert 2 Galaxies in the Sloan Digital Sky Survey, AJ, 136, 1179

Beckman, V., & Shrader, C. 2011, Active Galactic Nuclei, Wiley-Vch, 47 (Equation 3.9)

Condon, J. J. 1992, Radio Emission from Normal Galaxies, ARA&A, 30, 575

Condon, J. J., Cotton, W. D., & Broderick, J. J. 2002, Radio Sources and Star Formation in the Local Universe, AJ, 124, 675

Filippenko, A. V., & Sargent, W. L. W. 1989, Discovery of an Extremely Low Luminosity Seyfert 1 Nucleus in the Dwarf Galaxy NGC 4395, ApJL, 342, L11

Greene, J. E., & Ho, L. C. 2004, Active Galactic Nuclei with Candidate Intermediate-Mass Black Holes, ApJ, 610, 722

Greene, J. E., & Ho, L. C. 2007, X-Ray Properties of Intermediate-Mass Black Holes in Active Galaxies, ApJ, 656, 84

Ho, L. C., & Ulvestad, J. S. 2001, Radio Continuum Survey of an Optically Selected Sample of Nearby Seyfert Galaxies, ApJS, 133, 77

Huang, S., Haynes, M. P., Giovanelli, R., et al. 2012, Gas, Stars, and Star Formation in ALFALFA Dwarf Galaxies, AJ, 143, 133

Hunter, D. A., Elmegreen, B. G., & Ludka, B. C. 2010, Galex Ultraviolet Imaging of Dwarf Galaxies and Star Formation Rates, AJ, 139, 447

Kormendy, J., & Richstone, D. 1995, Inward Bound—The Search for Supermassive Black Holes in Galactic Nuclei, ARA&A, 33, 581

McQuinn, K. B. W., Skillman, E. D., Dolphin, A. E., & Mitchell, N. P. 2015, Calibrating UV Star Formation Rates for Dwarf Galaxies from STARBIRDS, ApJ, 808, 109

Markwardt, C. B. 2009, Non-Linear Least-Squares Fitting in IDL with MPFIT, Astronomical Data Analysis Software and Systems XVIII, 411, 251

Nelson, C. H. 2000, Black Hole Mass, Velocity Dispersion, and the Radio Source in Active Galactic Nuclei, ApJL, 544, L91

Richards, G. T., Lacy, M., Storrie-Lombardi, L. J., et al. 2006, Spectral Energy Distributions and Multiwavelength Selection of Type 1 Quasars, ApJS, 166, 470

Reines, A. E., Sivakoff, G. R., Johnson, K. E., & Brogan, C. L. 2011, An Actively Accreting Massive Black Hole in the Dwarf Starburst Galaxy Henize2-10, Nature, 470, 66

Reines, A. E., & Deller, A. T. 2012, Parsec-Scale Radio Emission from the Low-Luminosity Active Galactic Nucleus in the Dwarf Starburst Galaxy Henize 2-10, ApJL, 750, L24

Reines, A. E., Greene, J. E., & Geha, M. 2013, Dwarf Galaxies with Optical Signatures of Active Massive Black Holes, ApJ, 775, 116

Volonteri, M. 2010, Formation of Supermassive Black Holes, A&ARv, 18, 279

Woo, J.-H., Yoon, Y., Park, S., Park, D., & Kim, S. C. 2015, The Black Hole Mass-Stellar Velocity Dispersion Relation of Narrow-Line Seyfert 1 Galaxies, ApJ, 801, 38

Yun, M. S., Reddy, N. A., & Condon, J. J. 2001, Radio Properties of Infrared-Selected Galaxies in the IRAS 2 Jy Sample, ApJ, 554, 803